JAST, Vol. 13, No. 1, pp. 57-65

JAST
Journal of Aerospace Science and Technology

Scientific-Research Article

Calculation of Nonlinear Normal Modes Using EPFM Method

Meysam Jelveh[1], Seyed Mojtaba Mousavi[2],Mohammad Hamayoun Sadr[3]*

1-3 Faculty of Aerospace Engineering, Amirkabir University of Technology, Tehran
* Postcode: 15875-4413, Hafez St., Tehran
Email: *Sadr@aut.ac.ir

In the last decade, nonlinear normal modes have attracted the attention of many researchers, and many methods and algorithms have been proposed to calculate them. Among the proposed methods, the combination of the shooting method and the continuation of the periodic solution is the strongest methods. However, the computational cost of the method has still limited its application. In this paper, an updated formula is used to reduce the computational costs of the method. Using this updated formula significantly reduced the computation time so that the computational speed of nonlinear normal modes increased tenfold. Also, as the power of nonlinear terms increases in the system, the efficiency of the updated formula increases. In order to evaluate the accuracy of the proposed method, a system with two degrees of freedom was studied, and it was observed that the results obtained are consistent with the results in other works.

Keywords: *Nonlinear Normal Modes, the Continuation of the Periodic Solution Method, Updated Formula*

Introduction

Nonlinear normal modes are powerful tools in the analysis of nonlinear systems. Until the 1990s, nonlinear normal modes were known as theoretical concepts until a new look was created with the work of Vakakis [1-3], Shaw and Pierre [4-6]. Many researchers have paid attention to this issue in the last decade, and numerous review articles on nonlinear normal modes have been presented [7-10]. The cornerstone of the definition of nonlinear normal mode was laid by *Lyapunov*. He proved that for a Hamiltonian system with n degrees of freedom that is not in a state of internal resonance, there are n periodic solutions around the equilibrium point of the system [11]. After him, many efforts were made in this field. Weinstein (1973) [12] and Moser (1976) [13] generalized Lyapunov's theory in the presence of internal resonance [12]. Kauderer was the first to offer quantitative methods for calculating nonlinear normal modes [14].

Today, there are two standard definitions of the nonlinear normal modes: Rosenberg defined nonlinear normal modes as synchronous periodic vibrations in stable systems [15]. This definition means that all parts of the system reach their extreme values simultaneously. Shaw and Pierre considered the characteristics of lack of change in nonlinear normal modes and defined nonlinear normal modes as invariant manifolds in phase space. This means that if a movement starts in this manifold, it stays in

1 Associate professor
2 PhD candidate
3 PhD candidate

Received Date: 05 March 2020
Accepted Date: 04 May 2020

it until the end. If a system is under internal resonance, some degrees of freedom move faster than others.

Kerschen et al. (2009) generalized Rosenberg's definition and defined nonlinear normal modes as periodic but not necessarily synchronous vibrations. Haller and Ponsioen (2016) generalized the definition of Kerschen et al. and defined nonlinear normal modes as recurrent motion with a discrete Fourier spectrum of frequencies [16].

Based on these two definitions, methods for calculating nonlinear normal modes are divided into two general categories: methods that calculate the invariant manifold directly and methods that deal with the periodic solution in nonlinear systems.

This paper considers the calculation of nonlinear normal modes using the Rosenberg definition. There are very powerful and complex mathematical methods for calculating periodic solutions in nonlinear systems [22, 23]. One of the first attempts to calculate nonlinear normal modes in the system's periodic solution was performed using numerical methods by Slater [24]. He used the sequential continuity method to calculate the system's periodic solution. Lee et al. used a combination of shooting method and sequential continuity to calculate nonlinear normal modes [25]. Kerschen et al. (2009) used a combination of shooting method and response continuity based on pseudo-arclength [26]. They successfully obtained nonlinear normal modes for discrete and continuous nonlinear stable systems [27]. Kuether et al. implemented the method proposed by Peeters et al. in Abaqus Software and calculated the normal nonlinear modes of a surface with geometric nonlinear behavior [28, 29]. Renson et al. calculated the nonlinear normal modes of a satellite's structure using the method of Peeters et al. And extracted the modal interaction in it. They also present experimental evidence for results [30].

In addition to the analysis of real structures, normal nonlinear modes have been used in other fields such as energy [31], nonlinear vibration absorbers [32, 33], updating nonlinear finite element models [34, 38], and finding faults in nonlinear structures [39].

Among the various methods for calculating nonlinear normal modes, the combination of shooting method and continuity based on pseudo-arclength has been widely used, and in many articles, they are considered the primary method for validating other methods. However, the computational cost of these methods is still a problem.

In this paper, the updated formula presented by Deuflhard et al. is used to reduce the computation time [40]. This algorithm is based on Deuflhard et al. called the efficient path following method (EPFM).

In the following, the theory of the method is presented, and then its efficiency is evaluated in the format of the analysis of a nonlinear system with two degrees of freedom.

Efficient path following method

This method is similar to the method proposed by Peeters et al. The difference is that this method uses an updated formula to reduce the computational cost of the algorithm. To use this method, it is necessary first to determine the periodic solution of the system at an energy level. Then, using the continuation of the periodic solution method based on pseudo-arclength, the changes of nonlinear normal modes are calculated with the changes of energy in the system. Therefore, this chapter is divided into two parts. In the first part, finding the periodic solution of the nonlinear system using the shooting method, and in the second part, the continuation of the periodic solution method based on pseudo-arclength will be reviewed.

Shooting method

In general, the methods of calculating the periodic solution of a system are divided into two general categories: frequency domain and time domain. The standard method in frequency is harmonic balance and its developed methods. In the field of time, standard methods are single shooting, multiple shooting, collocation, and finite differences.

The initial value problem becomes a two-point boundary value problem in time-domain methods. In these methods, an initial condition and a solution with periodicity are sought, so that formula (1) is accurate.

$$x(x_0, T) = x_0 \quad (1)$$

The single shooting method is one of the most widely used numerical methods for finding the periodic solution of dynamic systems due to its simple structure. This method has been used in many software packages such as CANDSYS/QA and LOCBIF [34, 35]. Another advantage of this method is that the single value matrix (Monodormy) is generated in the implementation process, which can quickly calculate the flocculation coefficients and check the stability of the desired periodic solution. The governing formula on the system in the state space is expressed as Formula (2) in which $\dot{Z}$ is the vector of state variables.

$$\dot{Z} = g(Z) \quad (2)$$

The field vector in formula (2) is defined as formula (3).

$$g(z) = \begin{bmatrix} \dot{x} \\ -M^{-1}[Kx + f_{nl}(x, \dot{x})] \end{bmatrix} \quad (3)$$

The dynamic response of the system to the initial conditions of $z = (o) = z_o = [x_o^T \dot{x}_o^T]$ is shown as $z(t) = z(t, z_o)$ to indicate the dependence of the system response to the initial conditions. The answer of $z_p(t, z_{po})$ is the system's periodic response if it satisfies the conditions of formula (4), in which T is the minimum period of the system.

$$z_p(t, z_{p0}) = z_p(t + T, z_{p0}) \quad (4)$$

The single shooting method numerically solves the problem of a two-point boundary value with periodic conditions in the form of formula 5.

$$H(T, z_{p0}) \equiv z_p(T, z_{p0}) - z_{p0} = 0 \quad (5)$$

H is the shooting function and shows the difference between the initial conditions and the system response at the moment T. In a trial and error process, the single shooting method finds the initial conditions and periodicity to satisfy the periodicity condition.

This method is based on direct temporal integration and the Newton-Raphson algorithm. In this way, a T and z_{p0} are first guessed as the initial conditions and the periodicity of the system response. Then the system response in the assumed periodicity T is calculated by direct integration using numerical methods such as Rang Kota or Newmark. Generally, the initial conjecture (z_{p0}, T) does not satisfy the periodic conditions. Newton-Raphson algorithm is used to correct the initial conjecture. Here's how to fix the initial conjecture using the Newton-Raphson algorithm.

Correction values of Δz_{p0}^0 and ΔT^0 are obtained by extending the Taylor shooting function. The Taylor expansion of the shooting function is represented in formula 6.

$$H(T, z_{p0}) + \left.\frac{\partial H}{\partial z_{p0}}\right|_{(T, z_{p0})} \Delta z_{p0}^0 + \left.\frac{\partial H}{\partial T}\right|_{(T, z_{p0})} \Delta T^0 + H.O.T = 0 \quad (6)$$

The initial conditions of z_{p0} and the periodicity T, which determine the periodic motion of the system, are obtained with formula 7.

$$z_{p0}^{(k+1)} = z_{p0}^{(k)} + \Delta z_{p0}^{(k)}$$
$$T^{(k+1)} = T^{(k)} + \Delta T^{(k)} \quad (7)$$

Where $\Delta z_{p0}^{(k)}$ and $\Delta T^{(k)}$ are calculated by formula 8:

$$\left.\frac{\partial H}{\partial z_{p0}}\right|_{(T^k, z_{p0}^k)} \Delta z_{p0}^k + \left.\frac{\partial H}{\partial T}\right|_{(T^k, z_{p0}^k)} \Delta T^k = -H(T^k, z_{p0}^k) \quad (8)$$

In formula 8, k is the iteration number in the shooting method. This process continues until the desired accuracy is obtained. The convergence condition of the response is considered to be the relative error of the periodic conditions [31]. This condition is expressed in formula 9, in which ε is the optimal accuracy for the convergence of the response.

$$\frac{\|H\|}{\|z_{p0}\|} = \frac{\|z(T, z_{p0}) - z_{p0}\|}{\|z_{p0}\|} < \varepsilon \quad (9)$$

Matrix $\frac{\partial H}{\partial T}\left|(T, z_{p0})\right.$ is obtained from formula 10.

$$\left.\frac{\partial H}{\partial T}\right|_{(T, z_{p0})} = \left.\frac{\partial z}{\partial t}\right|_{t=T} = g\left(z(T, z_0)\right) = g\left(z(0, z_0)\right) \quad (10)$$

Matrix $\left.\frac{\partial H}{\partial z_{p0}}\right|_{(T^k, z_{p0}^k)}$ is defined using formula 11.

$$\frac{\partial H}{\partial z_{p0}}\left(T, z_{p0}\right)=\left.\frac{\partial z(t, z_{p0})}{\partial z_{p0}}\right|_{t=T}-\frac{\partial z_{p0}}{\partial z_{p0}}= \\ =\left.\frac{\partial z(t, z_{p0})}{\partial z_{p0}}\right|_{t=T}-I \tag{11}$$

Therefore, to calculate $\left.\frac{\partial H}{\partial z_0}\right|_{(T, z_0)}$, the Jacobi matrix $J=\left.\frac{\partial z(t, z_0)}{\partial z_0}\right|_{t=T}$ must be calculated. Each element of the Jacobi matrix is defined by formula 12. In this regard, Z_i is the i^{th} factor of Z and Z_{oj} is the j^{th} factor of Z_0.

$$\frac{\partial H}{\partial z_{p0}}\left(T, z_{p0}\right)=\left.\frac{\partial z(t, z_{p0})}{\partial z_{p0}}\right|_{t=T}-\frac{\partial z_{p0}}{\partial z_{p0}}= \\ =\left.\frac{\partial z(t, z_{p0})}{\partial z_{p0}}\right|_{t=T}-I \tag{12}$$

This matrix shows the response changes at moment t in exchange for the changes in the initial conditions. There are two general methods for calculating this matrix: sensitivity analysis and finite difference. In this paper, the finite difference is used. The governing equation is solved under the following two initial conditions in the finite difference method. The answer, similar to each of these initial conditions, is shown by $z(T, z_0)$ and $z_k(T, z_0+\delta e_k)$, respectively.

$$z(0)=z_0 \tag{13}$$

$$z^k(0)=z_0+\delta e_k \tag{14}$$

In the above formula e_k is the k^{th} column of the identity matrix and δ is a small number. Finally, element of matrix $J=\left.\frac{\partial z(t, z_0)}{\partial z_0}\right|_{t=T}$ are obtained from formula 15:

$$J_{\downarrow k}=\frac{z(T, z_0+\delta e_k)-z(T, z_0)}{\delta} \tag{15}$$

As it turns out, the highest cost of this method is related to producing Jacobi matrix in every attempt. If the sensitivity analysis method is used, it is necessary to integrate the differential equations with n^2 variables. If the finite difference method is used, it is necessary to integrate for n times the governing equation on the system. The Jacobi matrix is calculated using one of these two methods to reduce its production time in the trial and error process in the first attempt. In other attempts, the Jacobi matrix is generated using the update formula. Deuflhard et al. propose equation 16 to calculate the Jacobian matrix. In this regard, K represents the number of attempts.

$$\left.\frac{\partial H}{\partial z_0}\right|^{k+1}=\left.\frac{\partial H}{\partial z_0}\right|^{k}+H^{k+1}\frac{\left(\Delta z_0^{k}\right)^{T}}{\left|\Delta z_0\right|} \tag{16}$$

By calculating the Jacobian matrix, a system of n equation and n+1 unknowns are obtained: n unknowns of Δz_0 and an unknown. As it turns out, ΔT is an indefinite system. This is because the periodic response of an autonomous system to the linear transfer of the time source is invariant. That is, if $z(t, z_0)$ is a periodic solution of the system, then $z(t+\tau, z_0)$ will be the periodic solution for any desired τ.

For the uniqueness of the system's response, a phase condition equation is added to this system of equations. In this paper, phase conditions are considered equal to zero velocities of degrees of freedom at the beginning of motion.

Finally, the shooting method leads to the system of equations in the form of formula 17. In this regard, $h(z_{p0}, T)=0$ is the equation of phase condition.

$$F(z_{p0}, T)=\begin{cases} H(z_{p0}, T)=0 \\ h(z_{p0}, T)=0 \end{cases} \tag{17}$$

Continuation of the periodic solution method based on pseudo arclength continuation

This paper uses the Continuation of the periodic solution method based on pseudo arclength continuation. This method is one of the most robust methods of periodic solution continuity and can easily cross the return points on the response curve. In this method, the subsequent response on the path is calculated from a known point on the response curve. This method has three steps. The first step is prediction. At this point, an initial conjecture is estimated for the next point. In the second stage, the initial conjecture is corrected. At this stage, the initial conjecture, estimated in the prediction stage, is corrected using the Newton-Raphson method. The third step is to determine the step length to estimate the initial conjecture of the subsequent response.

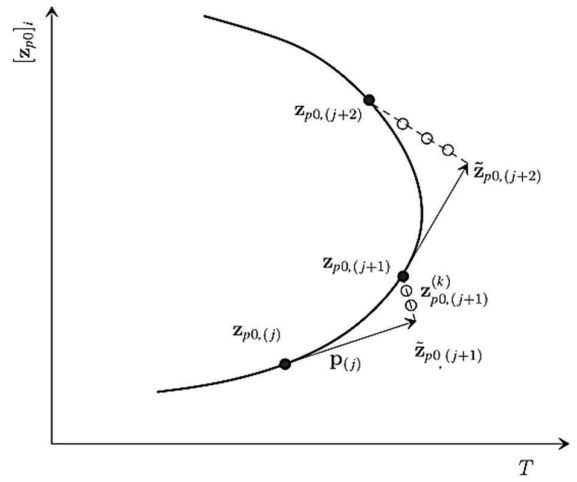

Figure 1: Continuation of the periodic solution method based on pseudo arclength continuation

The tangent method is used for prediction. In this method, the vector $P_{(j)}=\left[P^T_{z(j)}\,P_{T(j)}\right]^T$ is tangent to the path and is calculated by the following equation. In this regard, the method of calculating matrices of $\left.\frac{\partial H}{\partial z_{p0}}\right|_{(T_{(j)},z_{p0(j)})}$ and $\left.\frac{\partial H}{\partial T}\right|_{(T_{(j)},z_{p0(j)})}$ is the same as that described in the shooting method. h is also an equation of phase condition.

$$\begin{bmatrix} \left.\frac{\partial H}{\partial z_0}\right|_{(z_{p0(j)},T_{(j)})} & \left.\frac{\partial H}{\partial T}\right|_{(z_{p0(j)},T_{(j)})} \\ \left.\frac{\partial h}{\partial z_0}\right|_{(z_{p0(j)})} & 0 \end{bmatrix} \begin{Bmatrix} P_{z(j)} \\ P_{T(j)} \end{Bmatrix} = \begin{Bmatrix} 0 \\ 0 \end{Bmatrix} \quad (18)$$

One of its components is considered constant to calculate the tangent vector, and then the resulting system is solved using the Moore-Penrose method. It is then normalized using the formula $|\mathrm{p}|=1$ of normal tangent vector.

In the tangent method, the initial conjecture $\tilde{z}_{p0(j+1)},\tilde{T}_{(j+1)}$ is predicted for the next response $z_{p0(j+1)},T_{(j+1)}$ in the direction of the tangent vector in the given response $z_{p0(j)},T_{(j)}$. The relation of the predicted value is in the form of relation 19.

$$\begin{bmatrix} \tilde{z}_{p0(j+1)} \\ \tilde{T}_{(j+1)} \end{bmatrix} = \begin{bmatrix} z_{p0(j)} \\ T_{(j)} \end{bmatrix} + S_{(j)} \begin{bmatrix} P_{z(j)} \\ P_{T(j)} \end{bmatrix} \quad (19)$$

In this relation, $S_{(j)}$ is the step length in the direction of the tangent vector.

The initial conjecture, estimated in the prediction step, is then corrected using the Newton-Raphson method. In correcting the initial conjecture, to increase the convergence speed, the correction values of the initial condition and the periodicity is perpendicular to the calculated vector during the prediction step. The obtained $\tilde{z}_{p0(j+1)},\tilde{T}_{(j+1)}$ in the prediction step is used as the first conjecture. In the K^{th} attempt, the initial conditions and periodicity are obtained using formula 20. In this regard, k is the counter of each attempt in the correction process, and j is the counter of the response point on the curve.

$$\begin{aligned} z^{\,k+1}_{p0(j+1)} &= z^{\,k}_{p0(j+1)} + \Delta z^{\,k}_{p0(j+1)} \\ T^{\,k+1}_{(j+1)} &= T^{\,k}_{(j+1)} + \Delta T^{\,k}_{(j+1)} \end{aligned} \quad (20)$$

The values of the initial condition correction and the periodicity are calculated by solving the system of the following indeterminate equations using the Moore-Penrose method.

$$\begin{bmatrix} \left.\frac{\partial H}{\partial z_0}\right|_{(z^k_{p0(j+1)},T^k_{(j+1)})} & \left.\frac{\partial H}{\partial T}\right|_{(z^k_{p0(j+1)},T^k_{(j+1)})} \\ h(z^k_{p0(j+1)}) & 0 \\ P_{z(j+1)} & P_{T(j+1)} \end{bmatrix} \begin{Bmatrix} \Delta z^k_{p0(j+1)} \\ \Delta T^k_{(j+1)} \end{Bmatrix} = \begin{Bmatrix} -H\left(z^k_{p0(j+1)},T^k_{(j+1)}\right) \\ -h\left(z^k_{p0(j+1)}\right) \\ 0 \end{Bmatrix} \quad (21)$$

The main element in implementing an optimal and efficient periodic solution continuation method is step length control. There are several ways to control step length.

There are at least three factors that affect the length of the step, including:

Convergence behavior: The step length should be determined so that there is a suitable convergence speed in each step of correcting the initial conjecture.

Estimation of the response curve: The step length should be controlled so that small details of the response curve are also estimated.

Multi-branch: The step length should be chosen so that the multi-branch points on the response curve are well defined.

Of course, not all of the above factors are always taken into account to determine the length of the step. For example, the second factor is not considered in the homotopic method, where the

median responses are unimportant. On the other hand, when drawing the response curve of a system is important, the second factor must be considered. There are several ways to control step length. In this convergence behavior, the step of correcting the initial conjecture is considered. The step length in each step is selected so that the number of attempts in each correction step remains constant. Hence the step length in each step is determined using formula 22.

$$s^{j+1} = \frac{N_{opt}}{N_j} s^j \qquad (22)$$

In the above relation, s^{j+1} is the step length in the desired step, s^j is the step length in the previous step, N_{opt} is the number of desirable attempts in the correction stage and N_j is the number of attempts made in the previous correction step.

Numerical results

The nonlinear normal modes of the two-degree-of-freedom system were calculated to evaluate the accuracy and efficiency of the EPFM. Then, the results were compared with the results presented in [27]. Figure 2 shows the system under study.

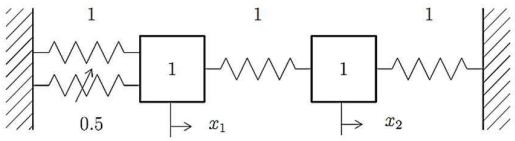

Figure 2: The two-degrees-of-freedom system

The governing equation of this system is in the form of formula (23):

$$\begin{aligned} \ddot{x}_1 + 2(x_1 - x_2) + 0.5x_1^3 = 0 \\ \ddot{x}_2 + (2x_2 - x_1) = 0 \end{aligned} \qquad (23)$$

In the EPFM method, the mode shape and frequency of the linear system are used as the initial conjecture to start the calculations. The shape of the mode and the linear frequency of this system are $\varphi = \begin{bmatrix} 1 & 1 \\ 1 & -1 \end{bmatrix}$ and $\omega^2 \begin{Bmatrix} 1 \\ 3 \end{Bmatrix}$, respectively, which are used to start calculations. The phase condition is such that the velocity components are set to zero at the beginning of the periodicity.

First, the system's behavior of nonlinear normal modes up to medium energy levels is investigated. Figure 3 shows the frequency-energy diagram of the first nonlinear normal mode of the system in question. As can be seen from the diagram, as the system energy increases, the frequency of the first nonlinear normal mode also increases. This is because the nonlinear spring in the system is of the third-degree type. Therefore, as the energy increases, the system's frequency increases, or in other words, the nonlinear spring becomes harder. Each of these nonlinear normal modes will be examined in more detail in the following. As can be seen, the results obtained from the EPFM method are in good agreement with the results obtained by Peeters et al. The results in this figure were obtained in 35 seconds by a computer with a 2.2 GHz corei7 CPU and 8GB of memory, without the use of an updated formula. In contrast, the updated formula reduces the calculation time to 9.5 seconds. This means that the EPFM method is 3.6 times faster.

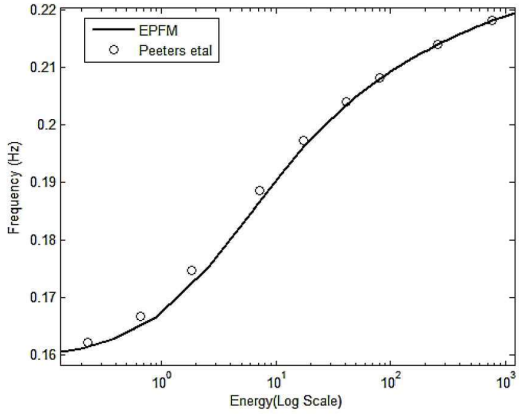

Figure 3: Frequency diagram of the energy of the first nonlinear normal mode up to the average energy levels

Figure 4 shows the modal curves of the first and second nonlinear normal modes. As shown in the figure, the modal curve is a straight line at very low energy levels. Gradually, as the energy level increases, this curve goes out of linear shape and becomes a curve. Another critical point that can be seen well in this figure is that with increasing the system's energy level, the amplitude of the second degree of freedom vibrations in the first nonlinear normal mode increases more than the amplitude of the first degree of freedom of the system. In other words, as the energy level increases, the first nonlinear normal mode is localized, meaning that most of the vibration energy is concentrated in the second degree of freedom. The opposite is true in the second nonlinear normal mode, with most of the vibrational energy concentrated in the first degree of freedom.

Figure 5 shows the nonlinear normal modes of the system at higher energy levels. The frequency of both modes increases with increasing energy. In the frequency-energy curve of the first mode, three tongues are observed. These tongues indicate the occurrence of internal resonance in this mode.
Figure 6 shows the first nonlinear normal mode at higher energy levels. The EPFM method needs 255 seconds to extract the first modal interaction. However, if the updated formula is not used, it will take 2647 seconds to obtain similar results. It takes 2683 seconds to calculate all three modal interactions using EPFM. Otherwise, it takes 15408 seconds to obtain these results.

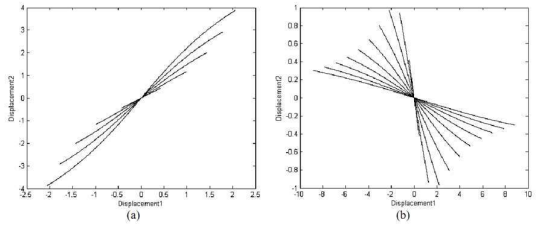

Figure 4: Modal curve of the first (a) and the second (b) nonlinear normal mode

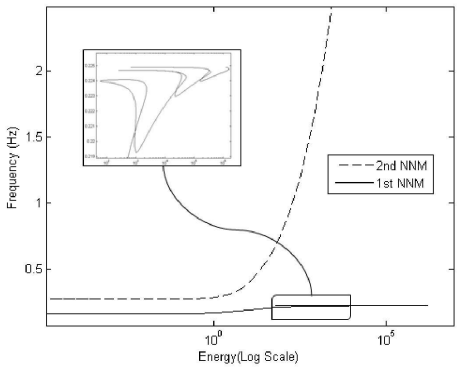

Figure 5: Energy-frequency diagram of the first and second nonlinear modes at high energy levels

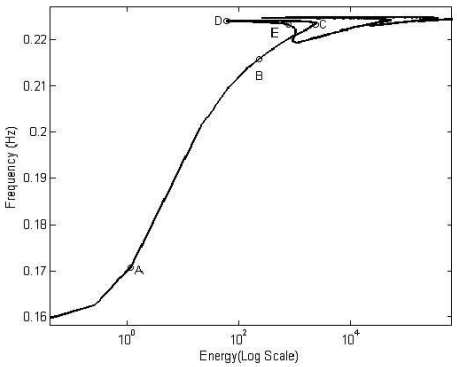

Figure 6: Energy-frequency diagram of the first nonlinear normal mode at high energy levels

Figure 7 shows these tongues in more detail. These tongues represent internal resonance in ratios of 1:3, 1:5, and 1:7, respectively. As can be seen, the results are very consistent with the results in [27].
Figure 8 shows the system's time response before and after internal resonance. As can be seen, the system response is no longer synchronized after modal interaction.

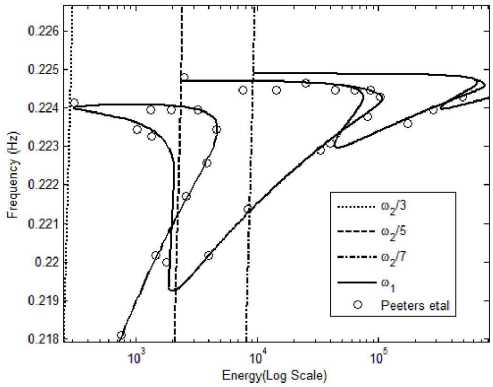

Figure 7: Details of modal interaction in the first nonlinear normal mode

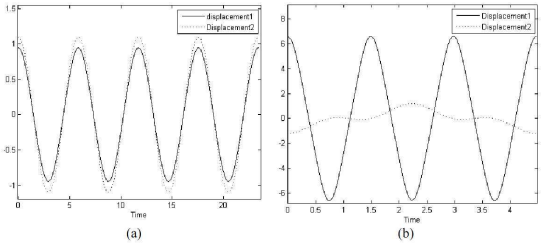

Figure 8: Time response diagram before (a) and after (b) modal interaction

Figure 9 shows the frequency response of the system's first and second nonlinear modes before and after the internal resonance. As can be seen at low energy levels, there is only one harmonic in each nonlinear mode, which is well spaced apart.

Gradually with increasing energy, the power of the third harmonic increases in the first nonlinear mode. Of course, this harmonic is still far from the first harmonic of the second mode. By further increasing the energy, the power of the third harmonic in the first nonlinear mode increases, and the power of the first harmonic decreases until the first harmonic disappears entirely in the internal resonance and the frequency of the third harmonic of the first mode equals the first harmonic frequency of the second mode. After internal resonance, the first harmonic of the first nonlinear mode appears again, but this time its power is less than the third harmonic.

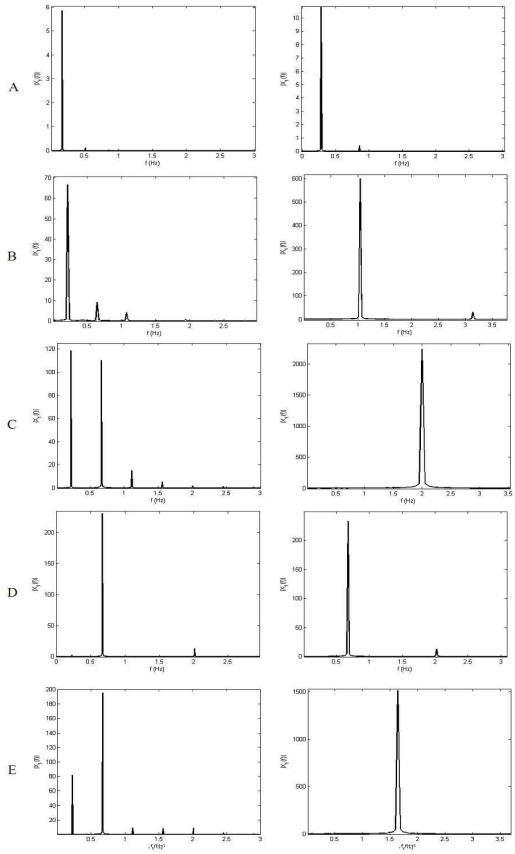

Figure 9: Frequency response of the first mode (left) and the second mode (right) before and after internal resonance

Numerical results

This paper presents a new algorithm based on the optimal path tracking method (EPFM) for calculating nonlinear normal modes. In order to increase the computational speed in this algorithm, an updated formula was used in calculating the Jacobi matrix. In order to evaluate the accuracy and efficiency of this algorithm, a two degrees-of-freedom nonlinear system was investigated. The results obtained are very consistent with the results presented in other sources. Also, the EPFM method is ten times faster than a similar method. The results also show that the higher the system's nonlinearity, the higher the efficiency of this method.

References:

[1] A.F. Vakakis, Analysis and identification of linear and nonlinear normal modes in vibrating systems, in: Mechanical engineering, California Institute of Technology, California, 1991.
[2]A.F. Vakakis, Non-similar normal oscillations in a strongly non-linear discrete system, Publisher, City, 1992.
[3]A.F. Vakakis, L.I. Manevitch, Y.V. Mikhlin, V.N.P. Chuk, A.A. Zevin, Normal Modes and Localization in Nonlinear Systems John Wiley & Sons, 1996.
[4] S. Shaw, C. Pierre, Non-linear normal modes and invariant manifolds, Publisher, City, 1991.
[5]S. Shaw, C. Pierre, On nonlinear normal modes., Publisher, City, 1992.
[6]S.W. Shaw, C. Pierre, Normal modes for non-linear vibratory systems, Publisher, City, 1993.
[7]Y.V. Mikhlin, K.V. Avramov, Nonlinears Normal Modes for Vibrating Mechanical Systems. Review of Theoretical Developments, Publisher, City, 2011.
[8]K.V. Avramov, Y.V. Mikhlin, Review of Applications of Nonlinear Normal Modes for Vibrating Mechanical Systems, Publisher, City, 2013.
[9]L. Renson, G. Kerschen, B. Cochelin, Numerical computation of nonlinear normal modes in mechanical engineering, Publisher, City, 2016.
[10]J.P. Noël, G. Kerschen, Nonlinear system identification in structural dynamics: 10 more years of progress, Publisher, City, 2017.
[11]A.M. Lyapunov, The General Problem of the Stability of Motion, Publisher, City, 1947.
[12]A. Weinstein, Normal modes for nonlinear hamiltonian systems, Publisher, City, 1973.
[13]J. Moser, Periodic orbits near an equilibrium and a theorem by Alan Weinstein, Publisher, City, 1976.
[14]H. Kauderer, Nichtlineare Mechanik Springer- Verlag, 1958.
[15]R.M.Rosenberg, On Nonlinear Vibrations of Systems with Many Degrees of Freedom, Publisher, City, 1966.
[16]G. Haller, S. Ponsioen, Nonlinear normal modes and spectral submanifolds: existence, uniqueness and use in model reduction, Publisher, City, 2016.
[17]E. Pesheck, Reduced order modeling of nonlinear structural systems using nonlinear normal modes and invariant manifolds, in, The University of Michigan., 2001.
[18]S.W. Shaw, C. Pierre, Normal modes of vibration for non-linear continuous systems, Publisher, City, 1994.
[19]L. Renson, G. Deliége, G. Kerschen, An effective finite-element-based method for the computation of nonlinear normal modes of nonconservative systems, Publisher, City, 2014.
[20]G.I. Cirillo, A. Mauroy, L. Renson, G. Kerschen, R. Sepulchre, A spectral characterization of nonlinear normal modes, Publisher, City, 2016.

[21]S. Ponsioen, T. Pedergnana, G. Haller, Automated computation of autonomous spectral submanifolds for nonlinear modal analysis, Publisher, City, 2018.
[22]R. Seydel, Practical Bifurcation and Stability Analysis, 3rd ed., Springer-Verlag, New York, 2010.
[23] W. Govaerts, Numerical Methods for Bifurcations of Dynamical Equilibria, SIAM, 2000.
[24]J.C. Slater, A numerical method for determining nonlinear normal modes, Publisher, City, 1996.
[25]Y.S. Lee, G. Kerschen, A.F. Vakakis, P. Panagopoulos, L. Bergman, D.M. McFarland, Complicated dynamics of a linear oscillator with a light, essentially nonlinear attachment, Publisher, City, 2005.
[26]G. Kerschen, M. Peeters, J.C. Golinval, A.F. Vakakis, Nonlinear normal modes, Part I: A useful framework for the structural dynamicist, Publisher, City, 2009.
[27]M. Peeters, R. Viguié, G. Sérandour, G. Kerschen, J.C. Golinval, Nonlinear normal modes, Part II: Toward a practical computation using numerical continuation techniques, Publisher, City, 2009.
[28]R.J. Kuether, M.S. Allen, A numerical approach to directly compute nonlinear normal modes of geometrically nonlinear finite element models, Publisher, City, 2014.
[29]R.J. Kuether, B.J. Deaner, J.J. Hollkamp, M.S. Allen, Evaluation of Geometrically Nonlinear Reduced-Order Models with Nonlinear Normal Modes, Publisher, City, 2015.
[30]L. Renson, J.P. Noël, G. Kerschen, Complex dynamics of a nonlinear aerospace structure: numerical continuation and normal modes, Publisher, City, 2015.
[31]A.F. Vakakis, Designing a Linear Structure with a Local Nonlinear Attachment for Enhanced Energy Pumping, Publisher, City, 2003.
[32]K.V. Avramov, O.V. Gendelman, On interaction of vibrating beam with essentially nonlinear absorber, Publisher, City, 2010.
[33]M.A. Al-Shudeifat, N.E. Wierschem, L.A. Bergman, A.F. Vakakis, Numerical and experimental investigations of a rotating nonlinear energy sink, Publisher, City, 2017.
[34]M. Kurt, M. Eriten, D.M. McFarland, L.A. Bergman, A.F. Vakakis, Methodology for model updating of mechanical components with local nonlinearities, Publisher, City, 2015.
[35]S. Peter, A. Grundler, P. Reuss, L. Gaul, R.I. Leine, Towards Finite Element Model Updating Based on Nonlinear Normal Modes, in: G. Kerschen (Ed.) Nonlinear Dynamics, Volume 1, Springer International Publishing, Cham, 2016, pp. 209-217.
[36]D.A. Ehrhardt, M.S. Allen, T.J. Beberniss, S.A. Neild, Finite element model calibration of a nonlinear perforated plate, Publisher, City, 2017.
[37]C.I. VanDamme, M. Allen, J.J. Hollkamp, Nonlinear Structural Model Updating Based Upon Nonlinear Normal Modes, in: 2018 AIAA/ASCE/AHS/ASC Structures, Structural Dynamics, and Materials Conference, American Institute of Aeronautics and Astronautics, 2018.
[38]M. Song, L. Renson, J.-P. Noël, B. Moaveni, G. Kerschen, Bayesian model updating of nonlinear systems using nonlinear normal modes, Publisher, City, 2018.
[39] W. Lacarbonara, B. Carboni, G. Quaranta, Nonlinear normal modes for damage detection, Publisher, City, 2016.
[40]F.B. Deuflhard P, Kunkel P, Efficient Numerical Pathfollowing Beyond Critical Points, Publisher, City, 1987.